

## Modeling of cyclic bond deterioration in RC beam-column connections

Ricardo Picón-Rodríguez<sup>†</sup>

*Department of Structural Engineering, Lisandro Alvarado University, Barquisimeto, Venezuela*

Carlos Quintero-Febres<sup>‡</sup> and Julio Flórez-López<sup>‡†</sup>

*Department of Structural Engineering, University of Los Andes, Mérida, Venezuela*

*(Received May 2, 2005, Accepted April 20, 2007)*

**Abstract.** This paper presents an analytical model for RC beam-column connections that takes into account bond deterioration between reinforcing steel and concrete. The model is based on the Lumped Damage Mechanics (LDM) theory which allows for the characterization of cracking, degradation and yielding, and is extended in this paper by the inclusion of the slip effect as observed in those connections. Slip is assumed to be lumped at inelastic hinges. Thus, the concept of “slip hinge”, based on the Coulomb friction plasticity theory, is formulated. The influence of cracking on the slip behavior is taken into account by using two concepts of LDM: the effective moment on an inelastic hinge and the strain equivalence hypothesis. The model is particularly suitable for wide beam-column connections for which bond deterioration dominates the hysteretic response. The model was evaluated by the numerical simulation of five tests reported in the literature. It is found that the model reproduces closely the observed behavior.

**Keywords:** R/C wide beam-column connection; bond deterioration; reinforcement slip; pinching in behavior loops; bond strengths; lumped damage mechanics; inelastic hinges; slip hinge.

---

### 1. Introduction

The inelastic response of reinforced concrete structures to cyclic, earthquake-type, loading is characterized by the degradation of the restoring-force characteristics. This degrading-type hysteretic behavior is a very complex phenomenon that is influenced by many material and structural parameters. This behavior must be considered when designing or evaluating seismic-resistant reinforced concrete structures.

Predicting the inelastic response of reinforced concrete structures requires the adequate modeling of various significant aspects of member hysteretic behavior, such as stiffness degradation, strength degradation, and pinching of the load-deformation hysteretic loops. Pinching of the hysteretic loops

---

<sup>†</sup> Ph.D., E-mail: [rpicon@ucla.edu.ve](mailto:rpicon@ucla.edu.ve)

<sup>‡</sup> E-mail: [carlosq@ula.ve](mailto:carlosq@ula.ve)

<sup>‡†</sup> E-mail: [iforez@ucla.edu.ve](mailto:iforez@ucla.edu.ve)

is due to various factors. Among these factors cyclic bond deterioration between reinforcing steel and concrete is one of the most influential ones. This type of behavior is typical of reinforced concrete frame elements and connections but is especially notorious in wide beam-to-column connections.

This type of connections is formed in wide beam frame systems, also called Banded Floor Systems. These popular and cost effective structural systems with shallow, wide beams, wider than the supporting columns, have been recently shown, La Fave and Wight (1999) and Quintero-Febres and Wight (2001), to possess some potential as lateral load resisting systems.

Several analytical models have been proposed in the past to represent the hysteretic response of RC members and structures. Simple bilinear formulations were initially used to model hysteretic response as it was presented by Aoyama (1964). A degrading bilinear model was introduced by Clough and Johnston (1966). A general tri-linear model was proposed by Takeda *et al.* (1970). This model, based on the results of several experimental studies, became widely accepted among researchers and has served as the basis for many other formulations. These models did not incorporate the pinching effect in the response. Other degrading models, some of them based on Takeda's model, which did not incorporate the pinching effect either, have been proposed (Saiidi and Sozen 1979, Anderson and Towsand 1977).

Among the models that incorporated the pinching behavior are: Aoyama (1968); Iwan (1973), Nakata *et al.* (1978), Roufaiel and Meyer (1983), the "three parameter" model by Park *et al.* (1987). Pinching behavior is typically incorporated by lowering the target maximum point for the reloading branches. In most cases, a user input "pinching parameter" must be used to help locate the pinching point.

The aforementioned models are defined based on key behavioral stages or points which define straight lines, and hence they are piecewise linear. This type of models has been named "polygonal hysteretic model", in contrast to "smooth hysteretic models", which are models "with continuous change of stiffness due to yielding but sharp changes due to unloading and deteriorating behavior", Sivaselvan *et al.* (2000). An example of this type is the Bouc's model (1967) that has been modified by other researchers and more recently by Reinhorn *et al.* (1995) and Gastebled (2000).

The work described in this paper focuses on the modeling of pinching in RC beam to column connections in which bond deterioration is major cause. This is particularly the case of wide beam-column connections. The mechanism of bond between concrete and reinforcing steel has been studied for decades. For most cases, bond properties have been obtained from tension tests. Anchorage slip or bond deterioration, one of the major components of inelastic deformation in reinforced concrete structures, has been analytically investigated by different authors as Soleimani (1979), Filippou and Issa (1988), Saatcioglu *et al.* (1992).

In this paper, bond deterioration between reinforcing steel bars and concrete is modeled by means of Lumped Damage Mechanics. This theory is based on the methods of Fracture Mechanics, Continuum Damage Mechanics and the concept of plastic hinge. Lumped Damage Mechanics is a general framework that allows for the modeling of RC framed structures subjected to monotonic loadings, Flórez-López (1993) and Cipollina (1995), cyclic loadings, Perdomo *et al.* (1999), low cycle fatigue, Thomson *et al.* (1998). The basic idea is the introduction, per hinges, of damage variables that only characterize concrete cracking, and a plastic strain variable that simulates the plastic rotation due to yielding of reinforcing steel. These variables modify the strength and stiffness properties of the frame member. Damage evolution is described by using fracture or damage mechanics criteria. Thus, concepts such as the energy release rate of a plastic hinge, Griffith

criterion or Paris law of fatigue can be used to describe damage evolution. Plastic strain evolution is described by using a yield function that simulates the variation of the elastic domain during hysteretic or monotonic analysis. Elastic domain can be described by using different criteria such as linear or non-linear kinematics and isotropic hardening.

None of the aforementioned references on Lumped Damage Mechanics considers the pinching effect. The model presented in this paper extends the concepts of Lumped Damage Mechanics to include pinching in the hysteretic curves due to slip of beam longitudinal reinforcing steel in RC beam-column connections. Even though the model can be used to simulate the response of any RC beam-column connections, it is particularly suitable for wide beam-column connections. In this type of connections a significant part of the beam longitudinal reinforcement passes outside the column core thus originating bond condition poorer than for normal beam connections. The inelastic deformations due to slip of the reinforcement are lumped at the plastic hinges of wide beam elements. Thus, new concepts, such as “slip hinge” and “slip moment” are introduced. This slip hinge only deals with the permanent strains due bond deterioration between concrete and reinforcing steel in the beam-column connections, the other inelastic strains are taken into account in the plastic hinges. A general inelastic hinge that concentrates complex energy dissipation phenomena (cracking, slip and yielding) is then formulated. This complex behavior is simulated by the proposed model in a simplified manner. The model was implemented in a commercial structural analysis program as a new finite element. The new software is used to simulate some experimental tests both on wide beam-column connections and on normal beam-column connections obtained literature. Thus, new parameters used in the model and the behavior of beam-column connections are evaluated.

## 2. Lumped damage mechanics

### 2.1 Notation

Let us consider a planar frame as shown in Fig. 1(a). The degrees of freedom of node  $j$  of the frame are given by the matrix  $\mathbf{u}_j^t = (u_j, v_j, \theta_j)$ , where the symbols  $u_j$ ,  $v_j$ , and  $\theta_j$  have the interpretation given in Fig. 1(b) and the letter “ $t$ ” indicates “transpose”.

Let us now consider a frame member  $b$  between the nodes  $i$  and  $j$ . The “displacement” matrix of this member is given by:  $\mathbf{q}_b^t = (\mathbf{u}_i^t, \mathbf{u}_j^t)$ . It can be noticed that the displacement variable does not establish differences between rigid body movements and modifications of the member shape. Thus, a “strain” matrix is introduced as follows:  $\Phi^t = (\phi_i, \phi_j, \delta)$ , where the variables  $\phi_i$  and  $\phi_j$  represent relative rotations with respect to the chord  $i-j$  and  $\delta$  is the elongation of the chord (see Fig. 1(c)). The relationship between displacements and strains is given by

$$\begin{aligned} \dot{\phi}_i &= \frac{\sin \alpha_{ij}}{L_{ij}} \dot{u}_i - \frac{\cos \alpha_{ij}}{L_{ij}} \dot{v}_i + \dot{\theta}_j - \frac{\sin \alpha_{ij}}{L_{ij}} \dot{u}_j + \frac{\cos \alpha_{ij}}{L_{ij}} \dot{v}_j \\ \dot{\phi}_j &= \frac{\sin \alpha_{ij}}{L_{ij}} \dot{u}_i - \frac{\cos \alpha_{ij}}{L_{ij}} \dot{v}_i - \frac{\sin \alpha_{ij}}{L_{ij}} \dot{u}_j + \frac{\cos \alpha_{ij}}{L_{ij}} \dot{v}_j + \dot{\theta}_j; \quad \text{i.e.,} \quad \dot{\Phi} = \mathbf{B} \dot{\mathbf{q}} \\ \dot{\delta} &= -\dot{u}_i \cos \alpha_{ij} - \dot{v}_i \sin \alpha_{ij} + \dot{u}_j \cos \alpha_{ij} - \dot{v}_j \sin \alpha_{ij} \end{aligned} \quad (1)$$

Where  $\mathbf{B}$  is called the transformation matrix and depends on the member displacements.

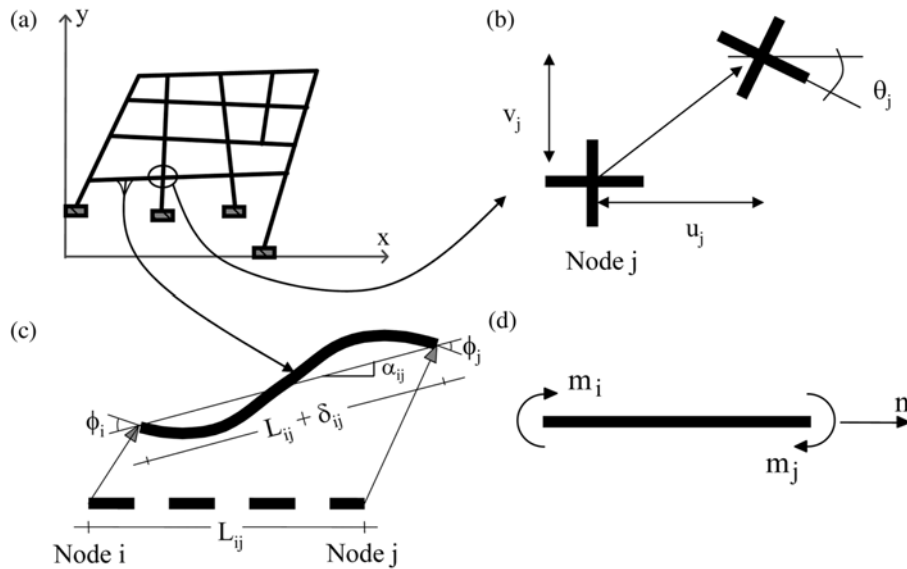


Fig. 1 (a) Planar frame, (b) Nodal degrees of freedom, (c) Generalized strains, (d) Generalized stresses

The internal or deformation power  $P_{int}$  of each element of a frame can be defined by the introduction of the “stresses”  $\mathbf{M}^t = (m_i, m_j, n)$ , where the meaning of the terms in  $\mathbf{M}$  is illustrated in Fig. 1(d).

$$P_{int} = \dot{\Phi}^t \mathbf{M} = \dot{\mathbf{q}}^t \mathbf{Q} \quad \text{where} \quad \mathbf{Q} = \mathbf{B}^t \mathbf{M} \quad (2)$$

The matrix  $\mathbf{Q}$  has the nodal forces of the frame member. The equilibrium equation can be obtained by the virtual power theorem, using the conventional expressions for the external and the inertial powers

$$\sum_{e=1}^n \mathbf{Q}_e + \mathbf{I} = \mathbf{P} \quad (3)$$

where  $n$  is the number of elements in the frame,  $\mathbf{I}$  represents the inertial forces and  $\mathbf{P}$  the external forces.

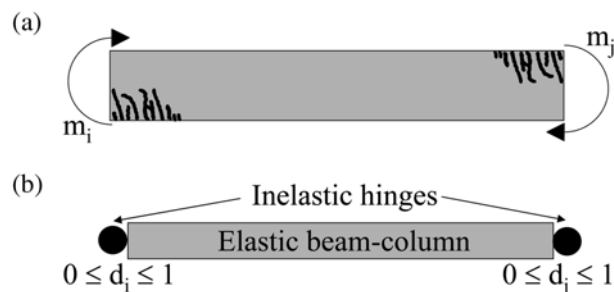


Fig. 2 (a) Lumped dissipation model and cracking state represented by internal variables, (b) Modeling of a frame structure

## 2.2 Constitutive law for a damaged frame member

A constitutive model for a frame member is the relationship between the history of stresses and the history of strains. The inelastic behavior of a frame member is represented by using the conventional lumped dissipation model. This model states that all energy dissipation in the frame member can be lumped at especial locations called “inelastic hinges”. Then, a frame member is assumed to be the assemblage of an elastic beam-column and two inelastic hinges located at its ends, such as shown in Fig. 2. Plastic rotations as well as concrete cracking will be lumped at the inelastic hinges.

Thus, the “plastic strain” matrix:  $\Phi_p^t = (\phi_i^p, \phi_j^p, 0)$  is introduced. The variables  $\phi_i^p$  and  $\phi_j^p$  are the plastic rotations of the inelastic hinges  $i$  and  $j$ . It can be noticed that the permanent elongation of the member is neglected. This is not a requirement of the model and it is assumed only for the sake of simplicity.

In Floréz-López (1998), the degree of concrete cracking was characterized by the introduction of a damage variable for the hinge that can take values between zero (no cracking) and one (total damage). Thus, the damage of a frame member is represented by the variable:  $\mathbf{D} = (d_i, d_j)$ , where the parameters  $d_i$  and  $d_j$  represent, respectively, the damage of the hinges  $i$  and  $j$ .

The stiffness and flexibility matrices of a damaged frame member can be written in terms of the damage variable as in Floréz-López (1998). Therefore, the elasticity law is given by

$$\Phi - \Phi_p = \mathbf{F}(\mathbf{D})\mathbf{M} \quad \text{and} \quad \mathbf{F}(\mathbf{D}) = \begin{bmatrix} \frac{F_{11}^0}{1-d_i} & F_{12}^0 & 0 \\ F_{21}^0 & \frac{F_{22}^0}{1-d_j} & 0 \\ 0 & 0 & F_{33}^0 \end{bmatrix} \quad (4)$$

The terms with the index 0 in Eq. (4) represent the elastic flexibility coefficients such as those presented in textbooks of structural analysis. It can be noticed that for a damage equal to zero, there is no additional flexibility. When the damage tends to one, the flexibility tends to infinity (or the stiffness tends to zero). In this way, stiffness degradation due to concrete cracking is represented. The complementary strain energy of a frame member is now given by

$$W^* = \frac{1}{2} \mathbf{M}^t \mathbf{F}(\mathbf{D}) \mathbf{M} \quad (5)$$

By analogy with the Theory of Fracture Mechanics, it is possible to introduce the energy release rate of a damaged hinge  $i$  in the following way

$$G_i = -\frac{\partial W^*}{\partial d_i} = \frac{m_i^2 F_{11}^0}{2(1-d_i)^2} \quad (6)$$

A “generalized Griffith criterion” can now be used to describe concrete cracking (or damage evolution in the plastic hinge  $i$ )

$$\begin{cases} \dot{d}_i = 0 & \text{if } G_i - R(d_i) < 0 \quad \text{or} \quad \dot{G}_i - \dot{R}(d_i) < 0 \\ \dot{d}_i > 0 & \text{if } G_i - R(d_i) = 0 \quad \text{and} \quad \dot{G}_i - \dot{R}(d_i) = 0 \end{cases} \quad (7)$$

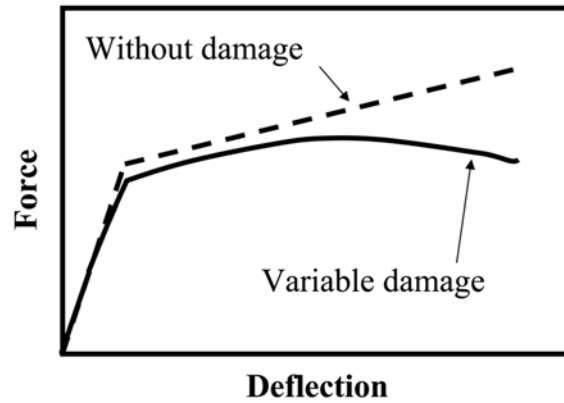


Fig. 3 Behavior of a plastic hinge with and without damage

Expression Eq. (7) states that damage (cracking) evolution is possible only if the energy release rate  $G$  reaches the value of the crack resistance  $R$ . The expression of the crack resistance of a plastic hinge, identified from experimental results, was proposed in Cipollina *et al.* (1995), see also Perdomo *et al.* (1999).

The yield function  $f^y$  of a damaged plastic hinge with kinematic hardening can be obtained using the concept of “effective moment on a plastic hinge” 1998. This concept is equivalent to the concept of effective stress that is used in soil mechanics and continuum damage mechanics. The effective moment hypothesis states that the behavior of a plastic hinge with damage can be obtained with the same expressions of a conventional plastic hinge if the moment is substituted by the effective moment, therefore for a hinge  $i$

$$f_i^y = \left| \frac{m_i}{1 - d_i} - c \phi_i^p \right| - k_y \leq 0 \quad (8)$$

where  $c$  and  $k_y$  are member dependent parameters. If the damage is kept constant, the yield function Eq. (8) and the state law Eq. (4) describe a bi-linear envelop in the moment-rotation or force-displacement curves. When the damage evolves, the constitutive law Eqs. (4)-(8) describes a behavior with a hardening phase after the yield moment of the cross section is reached, that ends in a maximum and a softening phase thereafter (see Fig. 3). The procedure to compute the parameters of the model as a function of the cross member properties can be seen in Perdomo *et al.* (1999).

### 3. Modeling of pinching due to reinforcement slip

#### 3.1 Interfaces with Coulomb friction plasticity

Consider an interface between two different continua as shown in the Fig. 4(a). Let  $\sigma$  and  $\tau$  be the normal and shear stresses on the interface. If the surface is characterized by a Coulomb friction criterion, the relative horizontal displacement  $h$  between the blocks obeys the following law

$$\begin{cases} \dot{h} > 0 & \text{if } |\tau| - \tau_s(\sigma) = 0 \\ \dot{h} = 0 & \text{if } |\tau| - \tau_s(\sigma) < 0 \end{cases} \quad (9)$$

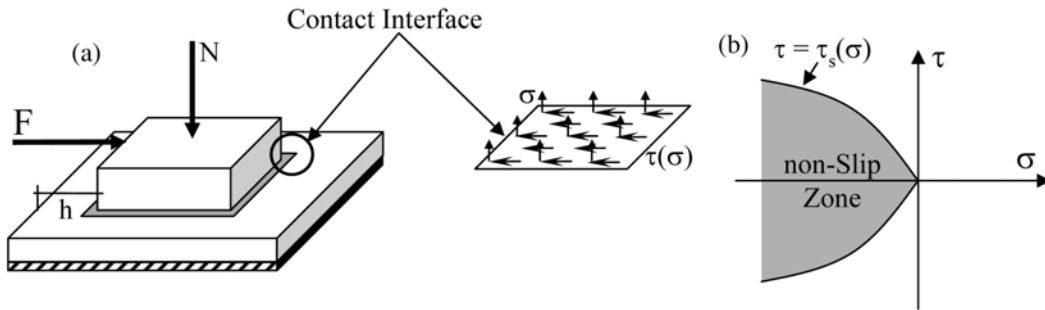


Fig. 4 (a) Interface between two media, (b) Non-slip convex

where the term  $\tau_s$  is the slip resistance that depends on the normal stress. The domain of non-slip, assuming an arbitrary resistance, is represented in the Fig. 4(b). It can be noticed that slip occurs when the shear stress reaches the value of the slip resistance. The latter value is not constant but depends on the normal stress. For higher values of the compressive normal stress, higher values of the slip resistance are obtained. A general presentation of interface behavior can be seen in plasticity textbooks, Salençon (1983).

### 3.2 Slip function of a plastic hinge

The process of slip of the reinforcement can also be explained in terms of Coulomb friction plasticity. In order to illustrate the slip process we will consider the case of interior plane beam-column joints, in which bond deterioration between concrete and reinforcement can be an important problem. Plane beams are elements wider than the supporting columns, in which a considerable part of the reinforcement passes outside the column core and thus, it is not as well confined as the reinforcement that passes through the column core is.

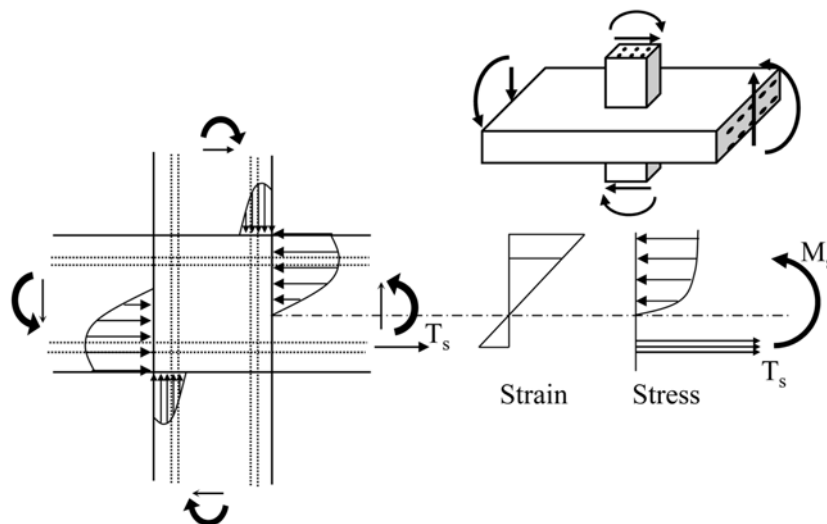


Fig. 5 Stress and strain distribution in an interior wide beam-column joint

Fig. 5 depicts an interior plane beam-column joint with low column axial load. In this case, the lower reinforcement is subjected to tractions on the right hand side and compression on the left side. In this situation for low values of the beam flexural moment, and low column compressions, the compression stresses on the interface between concrete and reinforcement in the beam plastic hinge region are very low and so is the slip resistance. Additionally the beam hoops are not contributing yet to the confinement of the concrete due to the little volumetric strains in the concrete. Therefore, small traction forces can produce slip of the reinforcement. For higher values of the moment, the hoops start to confine the concrete around the reinforcement and the compression stresses on the interface increase rapidly. The slip resistance grows faster than the tractions on the reinforcement and eventually, slip stops. Notice that in the case of an interior wide beam-column connection, the parts of the beam at the sides of the column do not have the column axial compression at all, and thus the phenomenon described above holds entirely.

In order to model this phenomenon, the lumped dissipation hypothesis will be used again, Fig. 2. Thus, it is assumed that slip of the reinforcement can also be lumped at the inelastic hinges. An inelastic hinge with slip generates plastic or inelastic rotations due to slip instead of yielding.

A generalization of the concept of Coulomb friction plasticity can be used to describe the behavior of an inelastic hinge with slip. Thus, the following “slip function” is introduced

$$f_i^s = |m_i| - k_s \leq 0 \quad (10)$$

Expression Eq. (10) must be interpreted as follows: there will be increments of the plastic rotations due to slip of the reinforcement if the hinge moment reaches the critical value  $k_s$ , otherwise these increments are nil.

As aforementioned, the slip resistance in the hinge is not constant, therefore neither is  $k_s$ . In this sense a slip hinge is similar to a plastic hinge. In order to model the increase in the yield moment in a plastic hinge, the Prager hypothesis was introduced in Eq. (8) (i.e., the use of a linear kinematic hardening term in the yield function). However, the Prager assumption is not adequate in the case of a slip hinge since it has been observed that slip resistance grows much faster than yield resistance. Therefore, in this paper, it will be assumed that the critical value  $k_s$  corresponds to a isotropic hardening function with an exponential term

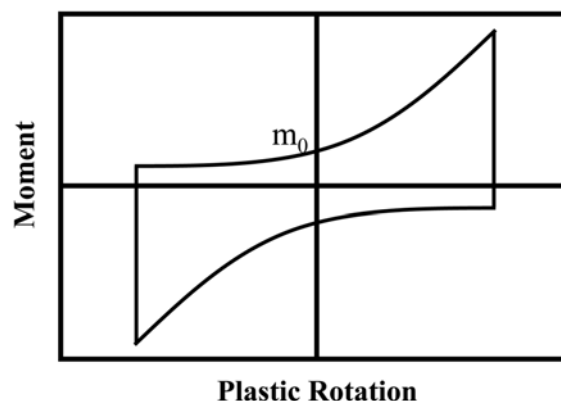


Fig. 6 Behavior of a slip hinge

$$k_s = m_0 \exp(\text{sign}(m_i) \gamma \phi_i^p) \quad (11)$$

The term  $m_0$  will be called “slip resistance” and is a concept similar to the yield moment in plasticity, i.e.,  $m_0$  is the moment that produces slip when no plastic rotations have occurred yet. The computation of the parameters  $m_0$  and  $\gamma$  will be discussed in the following sections. The behavior of a plastic hinge with slip with assumption (11) is represented in the Fig. 6. The use of an exponential term allows for the description of a slip resistance that grows very fast and tends to infinite for high values of the plastic rotation. It can be noticed that in this way, the pinching curves typical of the RC connection with slip of the reinforcement are obtained.

### 3.3 An inelastic hinge with slip and damage

Concrete cracking results in a reduction of the slip resistance in the plastic hinge region. The behavior of a slip hinge can be described by using again the concept of effective moment. Therefore, the slip function of an inelastic hinge with cracking is

$$f_i^s = \left| \frac{m_i}{1 - d_i} \right| - k_s \leq 0 \quad (12)$$

It can be noticed that the effective moment increases with the degree of cracking or equivalently, that the slip resistance decreases with cracking. Therefore smaller values of the hinge moment starts slip rotations.

### 3.4 The plasticity criterion in an inelastic hinge with slip or yielding

The yield function Eq. (8) describes a plasticity criterion of a plastic hinge whose physical mechanism is the yield of the reinforcement. The slip function Eq. (12) corresponds to a plasticity criterion of an inelastic hinge whose rotations are due to slip of the reinforcement. Of course, in a real wide beam-column joint, both mechanisms are possible and may occur one after the other. Physical evidence indicates that they do not occur at the same time Quintero-Febres and Wight 2001. Taking into account this observation, the following evolution law for the plastic rotations of an inelastic hinge with yielding and slip is proposed

$$\begin{cases} \dot{\phi}_i^p \neq 0 & \text{if } f_i = 0 \text{ and } \dot{f}_i = 0 \\ \dot{\phi}_i^p = 0 & \text{if } f_i < 0 \text{ and } \dot{f}_i < 0 \end{cases} \quad \text{where } f_i = \text{Max}(f_i^y, f_i^s) \quad (13)$$

It can be noticed that the new plasticity criterion determines what mechanism of plastic rotations is active, yield or slip, by the evaluation of the maximum value of both inelastic functions. If the maximum value is that of the yielding function, the plastic behavior will obey the kinematic hardening function defined by Eq. (8). On the other hand, if the maximum value is that of the slip function, the behavior will follow the exponential hardening function Eqs. (11) and (12). This criterion automatically changes from one mechanism to another as a function of the value of the moment, the plastic rotation and the specific properties of the cross section. Fig. 7 shows the behavior of an inelastic hinge that change from slip to yielding and vice versa in the case of constant damage.

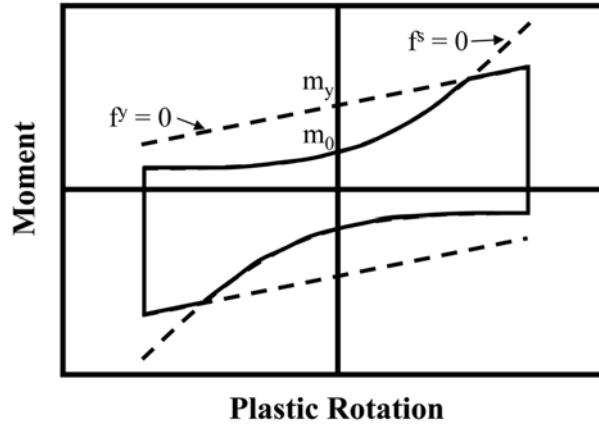


Fig. 7 Behavior of an inelastic hinge with slip and yielding

### 3.5 Determination of the slip resistance $m_0$

In the simulations that will be presented in section 4 of this paper, the parameter  $m_0$  was computed through the following simplified procedure.

Let us consider again the wide beam-column joint of Fig. 5. The strain distribution in the beam's cross section is assumed to follow the conventional linear distribution. The stress distribution also follows the usual parabolic diagram. Let us assume that the reinforcement in tension is subjected for the first time to the force  $T_s$  that produces slip and that no previous yielding has taken place. Then, the flexural moment  $m_s$  associated to  $T_s$  can be computed using strength of materials concepts. Under these conditions, the slip function Eq. (12) becomes

$$\frac{m_s}{1 - d_i} - m_0 = 0 \quad (14)$$

where  $d_s$  is the value of damage that characterizes the degree of cracking produced by the moment  $m_s$ . This value can be computed by the resolution of the damage law Eq. (7) for  $m = m_s$

$$\frac{m_s^2 F_{11}^0}{2(1 - d_s)^2} - R(d_s) = 0 \quad (15)$$

Therefore, expressions Eqs. (14)-(15) allow for the determination of  $m_0$  as a function of  $m_s$  or more precisely, as a function of the force  $T_s$ . This force can also be computed by conventional methods

$$T_s = \tau_s \cdot \pi \cdot d \cdot \ell \quad (16)$$

where  $\tau_s$  is the average slip stress,  $d$  the diameter of the bar and  $\ell$  the slip length. The stress  $\tau_s$  can be obtained by any of the accepted methods, Nielsen 1999 and Nilson 1991. In the examples of section 4, the lengths  $\ell$  indicated in Fig. 8 were used for interior connections.

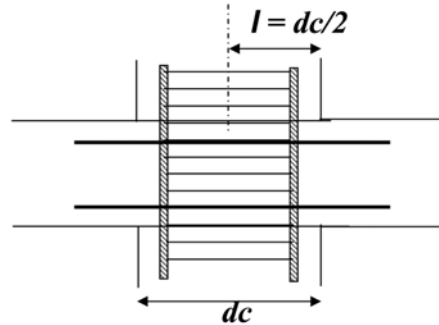


Fig. 8 Slip length for interior wide beam-column joints

### 3.6 Determination of $\gamma$

The last parameter needed for practical applications of the described model is  $\gamma$ . This parameter determines the point of intersection between the slip curve and the yield curve (see Fig. 9). As a result, the term  $\gamma$  can be written as a function of the damage:  $\gamma = \gamma(d)$  and can be obtained as follows. In the intersection point between both curves, all the expressions Eq. (17) hold

$$f^y = f^s = 0 \quad \text{and} \quad G = R(d) \tag{17}$$

Therefore, from these three equations the following expression of  $\gamma$  is obtained

$$\gamma(d) = \frac{1}{2} \frac{c(1-d) \ln \left( 2 \frac{R(d)(1-d)^2}{m_0^2 F^0} \right)}{\sqrt{\frac{2R(d)(1-d)^2}{F^0} - ck_y + cdk_y}} \tag{18}$$

It can be noticed that the parameter  $\gamma$  decreases with the damage variable. That is, a slip hinge with damage shows a slower recovery of the slip resistance during the process of confinement of the reinforcement.

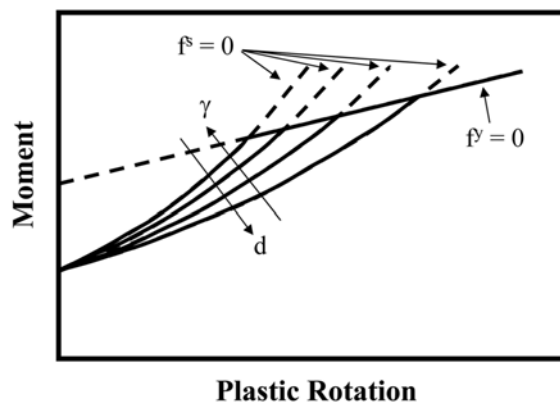


Fig. 9 Influence of the parameter  $\gamma$

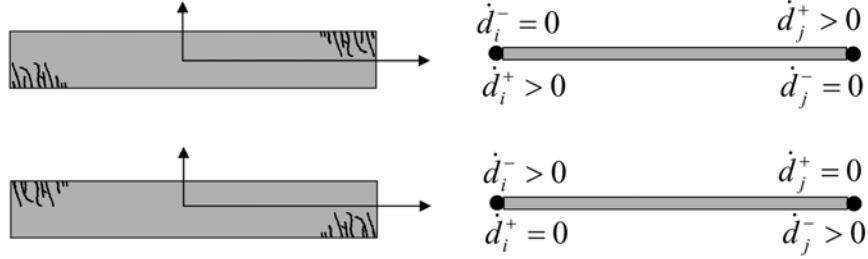


Fig. 10 Representation of cracking due to cyclic loading through damage variables

### 3.7 Unilateral effect and other extensions of the model

The model described in the previous sections can be improved by incorporating other concepts of continuum damage mechanics and fracture mechanics. It is particularly important the use of the unilateral damage idea.

In continuum damage mechanics, crack closure effects are represented by the introduction of two damage variables. One of them is related to microcracking density due to tensile stresses (positive damage) and the other represents damage due to compression stresses (negative damage). The stiffness of the material depends only on the positive damage variable if the stresses are positive and vice versa. Therefore, positive damage does not alter negative stiffness (positive cracks are assumed to be closed for negative stresses). In continuum damage mechanics, such a model is called “unilateral”.

The model described in this paper can include the concept of unilateral damage as described in Florez-Lopez 1998. In this generalization, two damage variables per hinge are introduced, one characterizes concrete cracking due to positive moments  $\mathbf{D}^+ = (d_i^+, d_j^+)$ , the other is related to negative moments  $\mathbf{D}^- = (d_i^-, d_j^-)$  (see Fig. 10).

The slip and yielding mechanisms described in the previous section can be easily adapted to the unilateral case. The state law Eq. (4) with two damage variables becomes

$$\Phi - \Phi_p = \mathbf{F}(\mathbf{D}^+) \langle \mathbf{M} \rangle_+ + \mathbf{F}(\mathbf{D}^-) \langle \mathbf{M} \rangle_- \quad (19)$$

where the symbols  $\langle m \rangle_+$  and  $\langle m \rangle_-$  mean, respectively, the positive part of  $m$  and the negative part of  $m$ . The damage evolution laws for hinge  $i$  are now

$$\begin{cases} \dot{d}_i^+ = 0 & \text{if } G_i^+ - R(d_i^+) < 0 \quad \text{or} \quad \dot{G}_i^+ - \dot{R}(d_i^+) < 0 \\ \dot{d}_i^+ > 0 & \text{if } G_i^+ - R(d_i^+) = 0 \quad \text{and} \quad \dot{G}_i^+ - \dot{R}(d_i^+) = 0 \\ \dot{d}_i^- = 0 & \text{if } G_i^- - R(d_i^-) < 0 \quad \text{or} \quad \dot{G}_i^- - \dot{R}(d_i^-) < 0 \\ \dot{d}_i^- > 0 & \text{if } G_i^- - R(d_i^-) = 0 \quad \text{and} \quad \dot{G}_i^- - \dot{R}(d_i^-) = 0 \end{cases} \quad (20)$$

where the energy release rates  $G_i^+$  and  $G_i^-$  are

$$G_i^+ = \frac{\langle m_i \rangle_+^2 F_{11}^0}{2(1 - d_i^+)^2}; \quad G_i^- = \frac{\langle m_i \rangle_-^2 F_{11}^0}{2(1 - d_i^-)^2} \quad (21)$$

Finally, the yield function Eq. (8) and the slip function Eq. (12) become

$$f_i^y = \max\left(\frac{m_i}{1-d_i^+} - c\phi_i^p; -\frac{m_i}{1-d_i^-} + c\phi_i^p\right) - k_y \leq 0 \quad f_i^s = \max\left(\frac{m_i}{1-d_i^+} - k_s^+; -\frac{m_i}{1-d_i^-} - k_s^-\right) \leq 0 \quad (22)$$

A second useful generalization is the use of modified Griffith criteria as those proposed in Thomson *et al.* (1998), Picón and Flórez-López (2000). These extensions allow for the consideration of low cycle fatigue effects that the original Griffith criterion does not.

#### 4. Model verification and numerical results

The behavior of a frame with damage, yielding and slip of the reinforcement is defined by the strain-displacement equation Eq. (1), the equilibrium equation Eq. (3), the state law Eq. (19), the damage evolution law Eq. (20), the plastic strain evolution law Eq. (13) and the yield and slip functions Eq. (22). Actually, the constitutive law Eqs. (19), (20), (13), (22) and the strain-displacement relationship define a finite element that can be included in the library of nonlinear structural analysis programs. This model was implemented in a commercial finite element program,

Table 1 Interior joint parameters

Specimen Design Parameter	Quintero and Wight (2001)	Hatamoto <i>et al.</i> (1991)	Kurose (1990)
$b_w/b_c$	1.85	<b>WB1</b> 1.77 <b>WB4</b> 3.57	0.80
Beam reinforcement	Top 5#5 + 2#4 $\rho = 0.53\%$ (1)	<b>WB1</b> 8-D10, $\rho = 1.70\%$ (2)	4#8, $\rho = 0.99\%$
	Bottom 4#5 + 2#4 $\rho = 0.45\%$	<b>WB4</b> 16-D10, $\rho = 1.69\%$	4#7, $\rho = 0.75\%$
% Anchored in column core	48%	<b>WB1</b> 50% <b>WB4</b> 25%	100%
$h/d_b(\text{beam})$ (3)	Top	22.4	<b>WB1</b> 20.3
	Bottom	28.0	<b>WB4</b> 20.3
Beam aspect ratio ( $b_w/b/h_b$ )	2.16	<b>WB1</b> 1.41 <b>WB4</b> 5.75	0.80
Column aspect ratio	1.0	<b>WB1</b> 1.0 <b>WB4</b> 1.0	1.0
Column axial load	No	<b>WB1</b> no <b>WB4</b> no	no
Column reinforcement	2.7%	<b>WB1</b> 3.53% <b>WB4</b> 3.53%	12#8, $\rho = 2.4\%$
$h/db$ (column)	19.2	<b>WB1</b> 12.6 <b>WB4</b> 12.6	20.0

(1) US reinforcement bar sizes (# $n = n/8$  in.; in = 25.4 mm)

(2) Japanese reinforcing bar sizes D10 (diameter = 0.39 in = 9.9 mm)

(3) ACI committee 352 recommended limit:  $h/db \geq 20$  (for normal beams) and  $h/db \geq 24$  (for wide beams)

(4) Column axial load divided by  $A_g f'_c$ , where  $A_g$  is the column cross section area.

Picón (1999), and the program was used to evaluate the performances of the model described in this paper by simulating the hysteretic response of five interior connections with wide and normal beams and one exterior wide-beam connection.

Table 1 shows the main design parameters for the interior test specimens used in the simulations.

#### 4.1 Interior wide beam-column connections

The numerical simulation of a test described in Quintero and Wight (2001) is presented in this section. The specimen, shown in Fig. 11(a), consisted in a wide beam-column connection subjected to quasi-static loadings that simulate earthquake solicitations. The boundary conditions and the structural representation for the analysis are indicated in Fig. 11(b). The experimental and numerical results are shown in Fig. 12. The parameters for the numerical simulation can be found in Vera (2002). Those parameters were the first cracking moment, yield moment, slip moment, ultimate moment, ultimate plastic curvature and the stiffness of each member of the structure. The damage distribution at the end of the simulation is shown in Fig. 13.

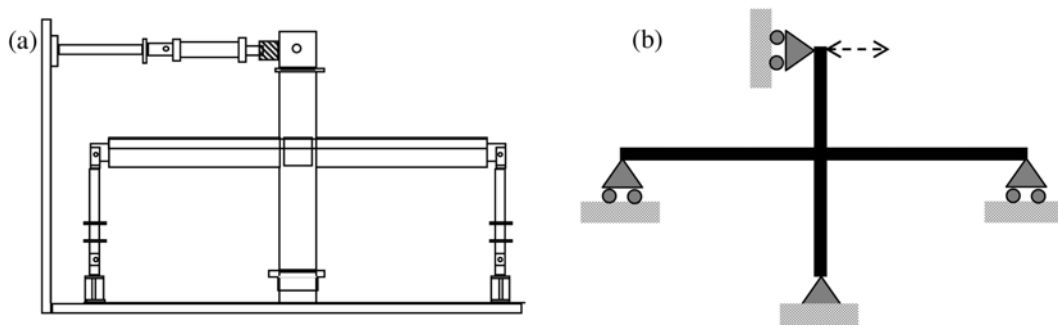


Fig. 11 (a) Test on an interior wide beam-column connection, (b) Boundary conditions for the analysis

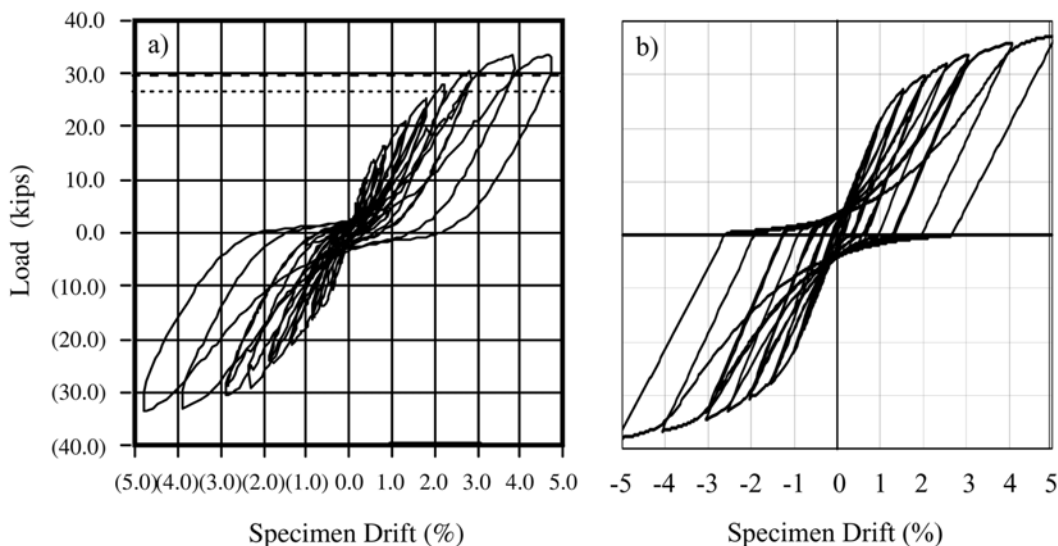


Fig. 12 Force vs. Displacement curves (a) Experimental results, (b) Numerical simulation

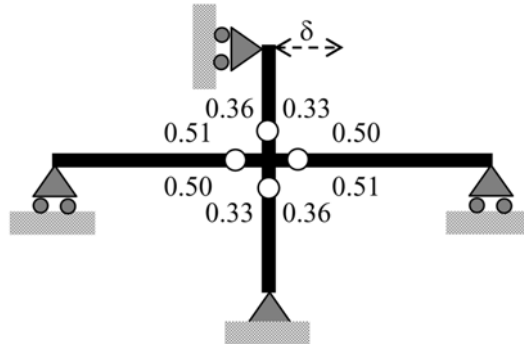
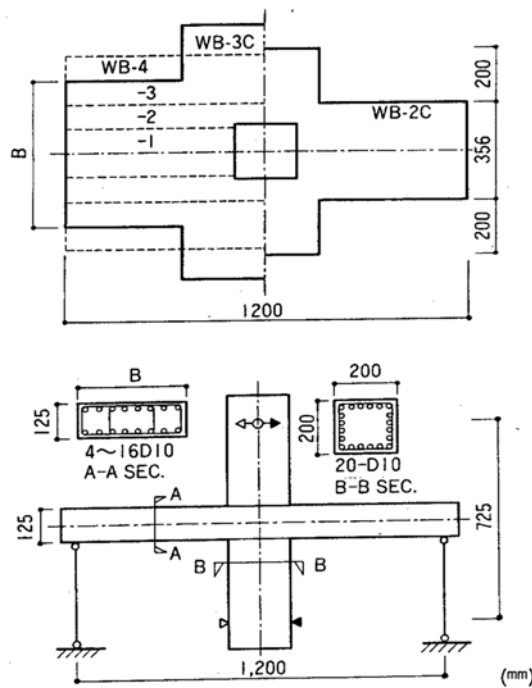


Fig. 13 Damage distribution at the end of the numerical simulation



Label	Db x Bb (in)	Dc x Bc (in)	Beam Rebars		Column Rebars	
			Long.	Trans.	Long.	Trans.
WB-1	4.9 x 6.9		4 D10	2 D-4 @ 2.0		
WB-2	4.9 x 14.0		8 D10	4 D-4 @ 2.0		
WB-3	4.9 x 21.1		12 D10	6 D-4 @ 2.0		
WB-4	4.9 x 28.2	7.9 x 7.9	16 D10	8 D-4 @ 2.0	20 D10	2 - $\phi$ 6

Diameter D10 = 0.39 in = 9.90 mm

Diameter D4 = 0.15 in = 3.81 mm

1 in = 25.4 mm

Fig. 14 Experimental test on four interior wide beam-column connections

Two other numerical simulations of experimental tests on interior wide beam-column connections are presented. The selected tests were chosen from an experimental program reported by Hatamoto *et al.* (1991). The test program consisted of four wide beam-column connections with different beam widths and other parameters kept constant. Fig. 14 shows the specimens dimensions and

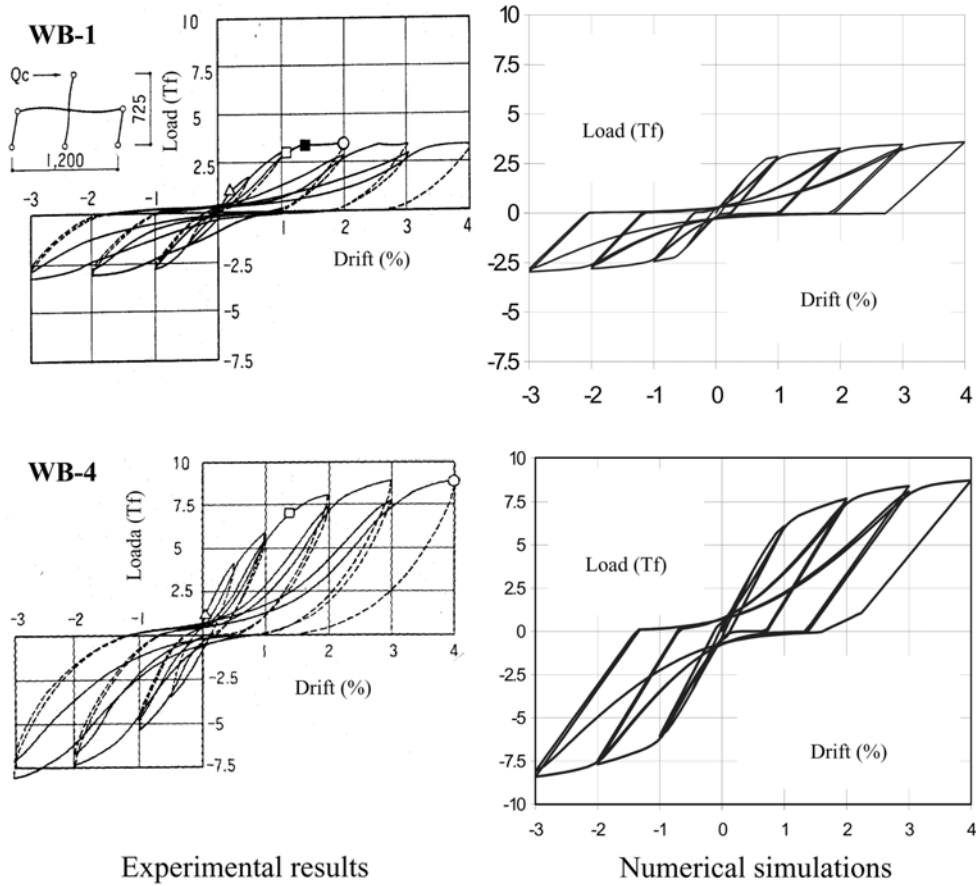


Fig. 15 Force vs. Displacement curves

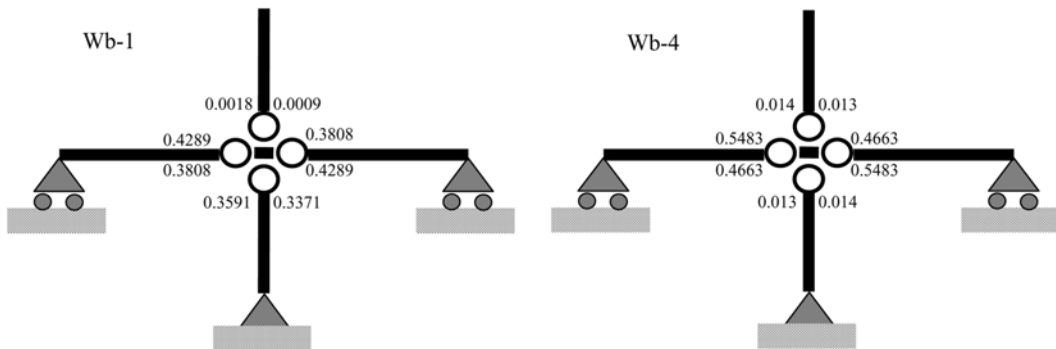


Fig. 16 Damage distribution at the end of the numerical simulation

reinforcement. The boundary conditions are the same as for the previous test (Fig. 11(b)). The parameters for each simulation were computed according to the method described in Vera (2002). The experimental and numerical curves for tests WB-1 and WB-4 are shown in Fig. 15, where the good agreement between experiment and simulation can be noticed. The Damage Model can show the damage maps, Fig. 16.

4.2 Interior normal beam-column connections

A numerical simulation of normal beam-column connections is shown in this section. The experimental tests were performed by Kurose (1990). Kurose’s experimental results and the corresponding simulation are presented in Fig 17. The simulation could not complete the analysis for the last cycle because the damage variables reached very high values (Fig. 17(c)). The simulation shows a behavior similar than the experimental test up to the point reached in the analysis though. It can be noticed that in that example there is very little pinching in both the experiment and the simulation. In the model, this is due to a high value of the parameter  $m_0$ , which is the consequence of the height of the specimen cross section (see Table 1). Therefore the model can simulate both behaviors and decide if pinching can be observed or not.

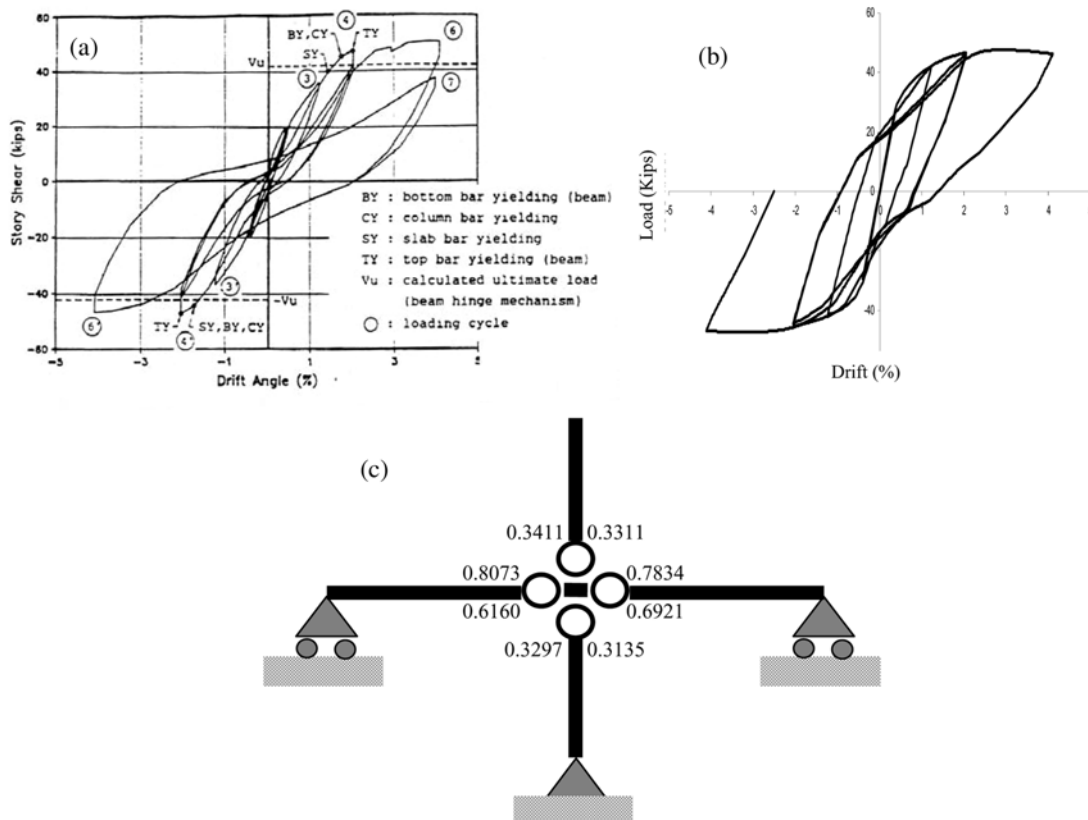


Fig. 17 Behavior curves of (a) Kurose 1990 experimental test, (b) simulation, (c) damage map

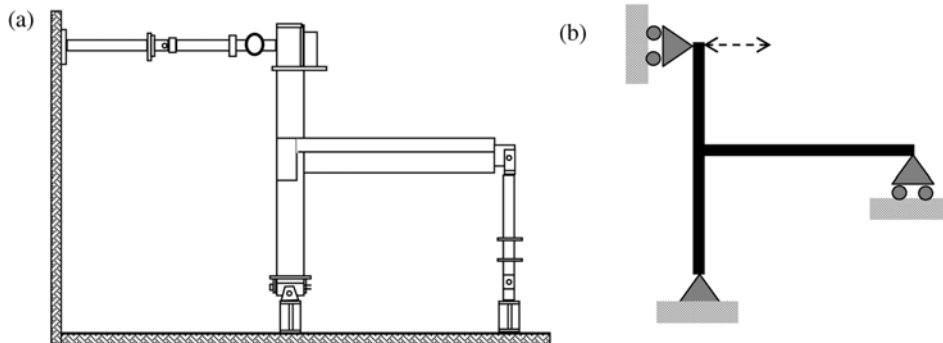


Fig. 18 (a) Test on an exterior wide beam-column connection, (b) Boundary conditions for the analysis

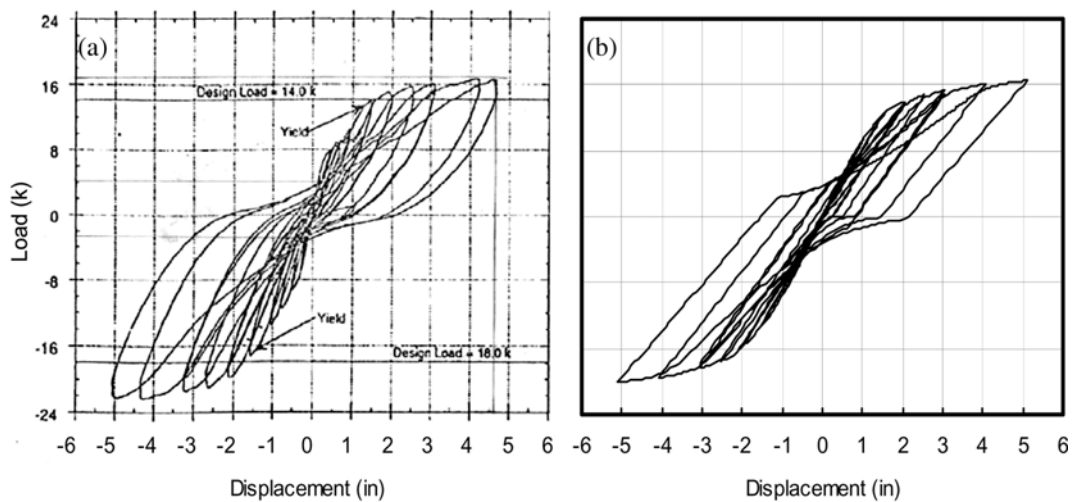


Fig. 19 Force vs. Displacement curves (a) Experimental results, (b) Numerical simulation

#### 4.3 Exterior connection case

This example corresponds to a test on an exterior joint with a wide beam reported by La Fave and Wight (1999). The specimen sketch is shown in Fig. 18(a) and the structural idealization in Fig. 18(b). Experimental and numerical results can be observed in Fig. 19.

#### 4.4 Simulation of an interior wide beam-column connection with and without considering bond deterioration

The model described in this work which considers the slip hinges into the lumped inelastic hinges allows representing the pinching effect on the force-displacement or moment-rotation curves. This was not possible with the previous version of the Lumped Damage Model, Perdomo *et al.* (1999) and Thomson *et al.* (1998). For comparison purposes, the first test shown in this paper was simulated using the lumped damage model with slip hinges (see Fig. 20(a)) and the previous version of the lumped damage model without slip hinges (see Fig. 20(b)). Fig. 20 shows that the

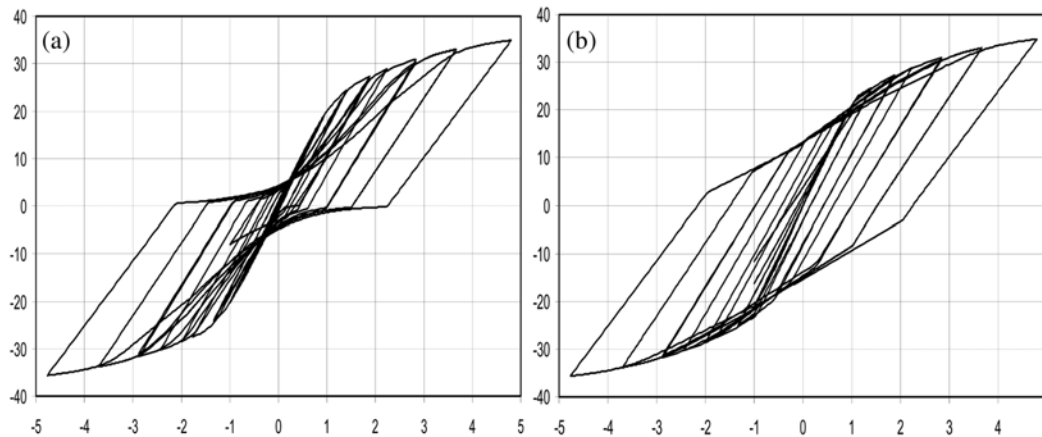


Fig. 20 Simulation of an interior wide beam-column connection (a) with and (b) without slip reinforcement

slip hinges, based on the theory of Coulomb friction plasticity, allow representing the pinching effect on the load-displacement curve while the previous model could not.

## 5. Conclusions

This paper presents an analytical model of the non-linear response of RC beam-column connections. The model includes the effect of cyclic bond deterioration on the shape of the force-displacement loops. In addition to the pinching effect, the model also considers the following effects: Stiffness and strength degradation due to concrete cracking, yielding of the reinforcement, plastic hardening in the reinforcement, degradation of the slip resistance due to concrete cracking in beam-column joints,  $P-\delta$  effects.

It has been assumed that the pinching in the force-displacement curves for beam-column connections is due to the transition from a behavior controlled by the slip of the reinforcement to a behavior governed by its yielding.

There is at least another important case where pinching is also observed: shear walls and short elements. However, in those cases pinching is due to the slip between two concrete blocks across a shear crack. This kind of phenomenon can also be modeled using Coulomb friction plasticity, but the damage model in this paper only considers flexure damage and no shear damage. Thus the present model can not be used in that case. However, any shear damage model valid for short elements could be modified in the same way as the proposed model.

The model reproduces the behavior observed during the tests reasonably well. The simplified procedure for the computation of the parameter  $m_0$  decreases the degree of pinching progressively as the height of the beam increases. This is in agreement with experimental observations. The reduction in the degree of pinching occurs because the values of  $k_s$  in the slip function approaches those of  $k_y$  in the yield function. Eventually, for high values of  $k_s$  slip is never present and there is no pinching in the curves.

The model tries to make an acceptable compromise between the necessary efficacy needed for engineering purposes and a concern for the development of a physically sounded description of the process.

## Acknowledgements

The results presented in this paper were obtained in the course of an investigation sponsored by FONACIT, CDCHT-ULA, and CDCHT-UCLA.

## References

- Anderson, J.C. and Towsand, W.H. (1977), "Models for RC frames with degrading stiffness", *J. Struct. Div.*, ASCE, **103**(ST12), 2361-2376.
- Aoyama, H. (1964), "Moment curvature characteristics of reinforced concrete members subjected to axial load and reversal of bending", *Proc. of the Int. Symposium on Flexural Mechanics of Reinforced Concrete*, Miami, Florida.
- Aoyama, H. and Sugano, T. (1968), "A generalized inelastic analysis of reinforced concrete structures based on tests of members", *Recent Researchs of Structural Mechanics – Contributions in Honor of the 60th Birthday of Prof. Y. Tsuboi, Uno Shoten*, Tokyo, Japan, 15-30.
- Bouc, R. (1967), "Forced vibration of mechanical systems with hysteresis", *Proc. 4th Conf. on Non-linear Oscillations*.
- Cipollina, A., López-Inojosa, A. and Flórez-López, J. (1995), "A simplified damage mechanics approach to nonlinear analysis of frames", *Comput. Struct.*, **54**(6), 1113-1126.
- Clough, R.W. and Jonston, S.B. (1966), "Effect of stiffness degradation on earthquake ductility requirements", *Proc. of Japan Earthq. Eng. Symp.*, October.
- Filippou, F.C. and Issa, A. (1988), "Nonlinear analysis of reinforced concrete frames under cyclic load reversals", *Report No. EERC-88/12, Univ. of California*, Berkeley, California, 120.
- Flórez-López, J. (1993), "Calcul simplifié de portiques endommageables", *Revue européenne des éléments finits/Eur. J. Finite Elem.*, **2**(1), 47-74.
- Flórez-López, J. (1998), "Frame analysis and continuum damage mechanics", *Eur. J. Mechanics A/Solid*, **17**(2), 269-284.
- Gastbled, O.J. and May, L.M. (2000), "Numerical simulation of pulled specimens", *ACI Struct. J.*, **97**(2), 308-315.
- Hatamoto, H., Bessho, S. and Matsuzaki, Y. (1991), "Reinforced concrete wide-beam-column subassemblages subjected to lateral load", *Design of Beam-Column Joints for Seismic Resistance*, SP 123. ACI. 291-315.
- Iwan, W.D. (1973), "A model for the dynamic analysis of deteriorating structures", *Proc. of 5th WCEE*, Rome.
- Kurose, Y. (1987), "Recent studies on reinforced concrete beam-column joints in Japan", PMFSEL report No. 87-8, Department Civil Engineering, The University of Texas at Austin, December.
- La Fave and Wight, J.K. (1999), "Reinforced concrete exterior wide beam-column slab connections subjected to lateral earthquake loading", *ACI Struct. J.*, 96-S64.
- Nakata, S., Sproul, T. and Penzien, J. (1978), "Mathematical modeling of hysteresis loops for reinforced concrete columns", *UCB/EERC Report 78-11*, University of California, Berkeley, June.
- Nielsen, M.P. (1999), *Limit Analysis and Concrete Plasticity*, CRS Press.
- Nilson, A.H. and Winter, G. (1991), *Design of Concrete Structures*, McGraw-Hill, Inc., New York.
- Park, Y.J., Reinhorn, A.M. and Kunnath, S.K. (1987), "IDARC: Inelastic damage analysis of reinforced concrete frame – shear-wall structures", *Tech. Rep. NCEER-87-0008*, State University of New York at Buffalo, Buffalo, N.Y.
- Perdomo, M.-E., Ramirez, A. and Florez-Lopez, J. (1999), "Simulation of damage in RC frames with variable axial forces", *Earthq. Eng. Struct. Dyn.*, **28**(3), 311-328.
- Picón, R. (1999), "Evolución de la degradación de rigidez en pórticos de concreto armado: implementación en abaqus del modelo histerético de daño considerando la fatiga de bajo ciclaje", (*In Spanish*) *M.Sc. Thesis University of Los Andes*, Mérida, Venezuela.
- Picón, R. and Flórez-López, J. (2000), "Evolución de la degradación de rigidez en pórticos de concreto armado" (*In Spanish*) *Proc. of XIX Jornadas Sudamericanas de Ingeniería Estructural*. Uruguay.

- Quintero-Febres, C. and Wight, J. (2001), "Experimental study of reinforced concrete interior wide beam-column connection subjected to lateral loading", *ACI Struct. J.*, **98**(4) 572-582.
- Reinhorn, A.M., Madan, A., Valles, R.E., Reichmann, Y. and Mander, J.B. (1995), "Modeling of masonry infill panels for structural analysis", *Tech. Rep. NCEER-95-0018*, State University of New York at Buffalo, Buffalo, N.Y.
- Roufaiel, M.S.L. and Meyer, C. (1983), "Analysis of damage concrete frames buildings", *Report No. NSF-CEE81-21359-1, Dept. of Civ. Engrg. and Engrg. Mech.*, Columbia Univ., New York.
- Saatcioglu, M., Alsiwat, J.M. and Ozcebec, G. (1992), "Hysteretic behavior of anchorage slip in RC members", *J. Struct. Eng.*, **118**(9), 2439-2458.
- Saiidi, M. and Sozen, M.A. (1979), "Simple and complex models for nonlinear seismic response of reinforced concrete structure", *Structural Research Series No. 465*, Civil Engineering Studies, University of Illinois, Urbana, Ill., Aug.
- Salençon J. (1983), "Calcul à la rupture et analyse limite" (in French), *Presses de l'école nationale des ponts et chaussées*, Paris.
- Sivaselvan, Mettupalayam V. and Reinhorn, Andrei M. (2000), "Hysteretic models for deteriorating inelastic structures", *J. Eng. Mech.*, **126**(6), 663-640.
- Soleimani, D., Popov, E.P. and Bertero, V.V. (1979), "Hysteretic behavior of reinforced concrete beam-column subassemblages", *ACI J.*, **76**(11), 1179-1195.
- Takeda, T., Sozen, M.A. and Nielsen, N.N. (1979), "Reinforced concrete response to simulated earthquakes", *J. Struct. Div.*, ASCE, **96**(ST12), 2557-2573.
- Thomson, E., Bendito, A. and Flórez-López, J. (1998), "Simplified model of low cycle fatigue for RC frames", *J. Struct. Eng.*, ASCE, **124**(9), 1082-1086.
- Vera, B. (2002), "Determinación de parámetros para un modelo de estrangulamiento por deslizamiento de refuerzo" (in Spanish). *M.Sc. Thesis, University of Los Andes, Venezuela.*